https://ntrs.nasa.gov/search.jsp?R=19810014461 2020-03-21T14:17:51+00:00Z

View metadata, citation and similar papers at core.ac.uk

brought to you by CORE

provided by NASA Technical Reports Serve

N O T I C E

THIS DOCUMENT HAS BEEN REPRODUCED FROM MICROFICHE. ALTHOUGH IT IS RECOGNIZED THAT CERTAIN PORTIONS ARE ILLEGIBLE, IT IS BEING RELEASED IN THE INTEREST OF MAKING AVAILABLE AS MUCH INFORMATION AS POSSIBLE

NGR-05-103-51
NSG-7105

Far-Infrared Rotational Emission by Carbon Monoxide

Christopher F. McKee*, J.W.V. Storey and Dan M. Watson

Department of Physics
University of California
Berkeley, California 94720

and

Sheldon Green

NASA Institute for Space Studies
2880 Broadway
New York, New York 10025

*Also, Department of Astronomy and Space Sciences Laboratory,
University of California, Berkeley.

(NASA-TM-82316) FAR-INFRARED ROTATIONAL EMISSION BY CARBON MONOXIDE (NASA) 29 p HC A03/MF A01 CSCL 03B

N81-22994

Unclas
G3/90 21381

ABSTRACT

Accurate theoretical collisional excitation rates are used to determine the emissivities of CO rotational lines for 10^4 cm^{-3} $\lesssim$ n(H_2), 100 K $<$ T $<$ 2000 K, and J $\lesssim$ 50. An approximate analytic expression for the emissivities which is valid over most of this region is obtained. Population inversions in the lower rotational levels occur for densities n(H_2) $\sim$ 10^{3-5} cm^{-3} and temperatures T $\gtrsim$ 50 K. Interstellar shocks observed edge-on are a potential source of millimeter-wave CO maser emission. The CC rotational cooling function suggested by Hollenbach and McKee (1979) is verified, and accurate numerical values given. Application of these results to other linear molecules should be straightforward.

I. INTRODUCTION

The development of far-infrared spectroscopy is opening a new window on the Universe. Rotational lines of astronomically abundant molecules often lie in the far-infrared. Observation of these lines provides a powerful probe for determining both the density and temperature of the emitting gas, as recently demonstrated by the interpretation of the observations of the J = 21 → 20, 22 → 21, 27 → 26, and 30 → 29 lines of hot CO in Orion (Watson et al 1980, Storey et al 1981). Using collisional excitation cross-sections calculated by one of us (S.G.), Storey et al (1981) calculated the CO rotational level populations and line intensities for a number of temperatures and densities and showed that the observed intensities in Orion could be modelled by emission from two components: a 2000 K component with $n(H_2) \simeq 1 \times 10^6$ cm^{-3} and a 400 - 1000 K component with $n(H_2) \simeq 5\text{-}2 \times 10^6$ cm^{-3}.

Inverting a 51 by 51 matrix to determine the level populations (as done by Storey et al) is somewhat cumbersome for interpreting data, and is completely impractical for theoretical calculations of the emission spectra of shocks, etc. In this paper accurate numerical results for the line intensities for optically thin CO collisionally excited by H_2 are presented for a number of points in the regime $n(H_2) > 10^4$ cm^{-3} and 100 K $< T <$ 2000 K (§II). In §III we use an approximation introduced by Hollenbach and McKee (1979; hereafter, HM) to obtain an analytic expression for the level populations and line intensities which is accurate to within a factor 1.3 over most of this regime. Since the theoretical collision cross-sections have an accuracy of about 30% and astronomical observations average over regions at a variety of temperatures and densities, the analytic approximation should be quite adequate for astronomical purposes. Inversion of the lower rotational levels is discussed in §IV. We also use the numerical results to evaluate the

accuracy of the CO cooling rate found by HM (§ V).

Although we have focussed on CO as the typically most abundant molecule other than H_2, our methods should also apply directly to other linear molecules such as HCN, HC_3N, and HCO^+.

II. EXACT CALCULATION OF POPULATIONS

Calculation of the equilibrium population of each state requires first of all a detailed knowledge of the entire matrix of collisional rate coefficients, $\gamma_{JJ'}$, from every state, J, to every other state, J'. Although such detailed information cannot yet be obtained experimentally, it has been possible to obtain fairly accurate values theoretically. This involves two steps, computing the intermolecular forces and then calculating the scattering dynamics. In an early study, Green and Thaddeus (1976) obtained the forces from a simple quantum mechanical model and solved for the dynamics by an essentially exact numerical method which is tractable only at very low collision energies where few rotational levels are accessible. Subsequently Green and Chapman (1978) extended these results somewhat by using approximate scattering techniques. In a more recent study, Thomas et al. (1980) have recomputed the intermolecular forces via accurate ab initio solution of the Schroedinger equation; these authors showed that the improved potential predicted state-to-state rates which differed in some cases by up to a factor of two from earlier values, although the total excitation rate did not change very much. As discussed by Green and Thomas (1980) available pressure broadening data can be used to provide some check on the theory, and, in fact, agreement is within experimental error.

At high energies, where many levels are accessible, the problem becomes unwieldy due to the number of state-to-state rates which must be considered. Fortunately, when the kinetic energy is large compared to the rotational

energy spacings, it can be shown that the various rates are not all independent; in particular the entire matrix of rates can be obtained simply in terms of one row γ_{J0} (Goldflam et al. 1977):

$$\gamma_{JJ'} = (2J'+1) \sum_{L} (2L+1) \begin{pmatrix} J & L & J' \\ 0 & 0 & 0 \end{pmatrix}^2 \gamma_{L0}, \quad J' < J \tag{2.1}$$

where $\begin{pmatrix} J & L & J' \\ 0 & 0 & 0 \end{pmatrix}$ is the usual three-j symbol. Eq. (2.1) applies only to downward rates, but upward rates can be obtained from detailed balance,

$$\gamma_{J',J} = \gamma_{JJ'}[(2J+1)/(2J'+1)] \exp(-\Delta E/kT) \tag{2.2}$$

For a given collision energy, this approximation becomes less accurate for higher rotational levels since the energy splittings increase with increasing J. As shown by DePristo et al. (1970) one can approximately correct for this defect by a simple modification of Eq. (2.1) which takes into account the rotational energy splittings:

$$\gamma_{JJ'} = (2J'+1) \sum_{L} (2L+1) \begin{pmatrix} J & L & J' \\ 0 & 0 & 0 \end{pmatrix}^2 A(L,J)^2 \gamma_{L0}, \quad J' < J. \tag{2.3}$$

The correction factor is given by

$$A(L,J) = [6+\Omega(L)^2]/[6+\Omega(J)^2], \tag{2.4}$$

with

$$\Omega(n) = 0.13\, n\, B\, \ell\, /\, (\mu T)^{1/2}, \tag{2.5}$$

where the rotation constant B is in cm^{-1}, the collisional reduced mass μ is in atomic mass units, the kinetic temperature T is in kelvins, and the scattering length ℓ is in Å, with a typical value ℓ = 3Å.

The γ_{L0} needed in Equation (2.3) have been obtained from new scattering calculations. Using the accurate intermolecular forces of Thomas et al. (1980), we computed cross-sections at eleven collision energies ranging from 100 to 5000 cm^{-1} using the IOS scattering approximation, which has been shown to be accurate for this system (see Goldflam et al. 1977 and Green 1979). Rate constants γ_{L0} for L < 32 were obtained by averaging these cross-sections over

Boltzmann distributions of collision energies at the appropriate temperatures. The resulting values, which are given in Table 1, were then used with Eq. (2.3) to provide all the necessary collisional rates. (Note that γ_{LO} with L > 32 were set to zero.)

It should be noted, finally, that all of these calculations have specifically treated excitation of CO by collisions with He atoms. It has been argued (e.g. Green and Thaddeus 1976) that excitation by H_2 is quite similar, the main difference being the greater velocity of H_2 at a given temperature due to its smaller mass. This factor will increase the rates for H_2 excitation by about 50% from the values for He. Experimental evidence in support of this procedure can be found in available pressure broadening data (Nerf and Sonnenberg 1975; see also Brechignac et al 1980).

The population of each rotational state can now be calculated from the collisional rates $\gamma_{JJ'}$ by solving the equations of of statistical equilibrium for these states. For the particular case of shocked CO, certain simplifications can be made:

1) Each line is assumed to be optically thin.

2) Infrared pumping by dust emission is assumed to be negligible.

3) Only the ground vibrational state contains a significant population.

Observational evidence to date supports these assumptions. The equations of statistical equilibrium are set up as follows. In steady-state, the rate at which molecules leave each state is equal to the rate at which they enter it:

$$n_J(A_J + n(H_2) \sum_{J'} \gamma_{JJ'}) - (n(H_2) \sum_{J'} \gamma_{J'J} n_{J'} + n_{J+1} A_{J+1}) = 0 \qquad (2.6)$$

where n_J is the density of molecules in state J, $n(H_2)$ is the density of H_2 molecules, and A_J is the A-coefficient for a radiative transition from state J to J-1. There is one such equation for each rotational state J. Together with the normalizing condition, $\sum_J n_J = n(CO)$, these expressions make up a

complete set of linearly independent equations, the solution of which is straightforward.

In the optically thin case the line emission coefficient I_J for the transition J to J - 1 is given by:

$$I_J = \frac{h\nu}{4\pi} A_J \, n_J/n(CO) \quad [\text{erg sec}^{-1} \text{ molecule}^{-1} \text{ sr}^{-1}] \tag{2.7}$$

where ν, the transition frequency, is just 2J times the rotational constant B (neglecting centrifugal distortion). Figure 1 shows the line emission coefficients as a function of J for $J \leq 50$, at several temperatures and densities. These curves result from computer solution of the equations (2.6) with $J \leq 60$, as described above.

III. ANALYTIC ESTIMATE OF POPULATIONS

In order to make progress in obtaining an analytic estimate of the level populations of the CO molecule, it is necessary to make a drastic simplification in the collision cross-sections $\sigma_{JJ'}$ connecting levels J and J'. Here we follow HM and adopt

$$\gamma_{JJ'} = \langle \sigma_{JJ'} \, v \rangle = \frac{g_{J'} \exp(-E_{J'}/kT) \, \sigma v_T}{Z} \tag{3.1}$$

where Z is the partition function, $v_T = [8kT/\pi m(H_2)]^{1/2}$ is the mean speed of the H_2 molecules, $g_{J'} = 2J' + 1$ is the degeneracy of the state J', and σ is the total collision cross-section out of level J:

$$\sum_{J=0}^{\infty} \langle \sigma_{JJ'} \, v \rangle = \sigma v_T, \tag{3.2}$$

Equation (3.1) for the cross-section has the advantages that it satisfies detailed balance and it facilitates solution of the level population equations. Its major disadvantage is that it depends only on the final state

and therefore omits a conspicuous feature of the calculated cross-sections, namely that collisions with small ΔJ are strongly favored over those with large ΔJ (cf. Table 1). Numerical evaluation of σ shows that it is about 10^{-15} cm^2, as assumed by HM; the effective value required to determine the level population is smaller, as we shall see below. With expression (3.1) for the cross-section, equation (2.3) for the level populations readily simplifies to

$$n_J(A_J + \frac{1}{2}\, n\, \sigma\, v_T) = n_{J+1}\, A_{J+1} + \frac{1}{2}\, n\, n_J^*\, \sigma\, v_T \qquad (3.3)$$

where

$$n_J^* = n(CO)\, \frac{g_J\, e^{-E_J/kT}}{Z} \qquad (3.4)$$

is the LTE population, n is the number density of hydrogen nuclei, and $n(H_2) = n/2$ in a fully molecular gas. In deriving equation (3.3), we set $\sigma_{JJ} = 0$ although it is non-zero according to equation (3.1); we also set

$$\sum_{J' \neq J} n_{J'} \approx n(CO) \qquad (3.5)$$

Although in this paper we are focussing on the case of optically thin emission, it is a simple matter to include the effects of line opacity via the escape probability formalism (e.g., deJong 1973, HM). If $\epsilon_J < 1$ is the probability that a photon in the $J \rightarrow J-1$ transition can escape the emission region, then the transition probability A_J is replaced by $A_J\, \epsilon_J$ in equation (3.3). Making this substitution, we introduce

$$a_J \equiv \frac{2A_J\, \epsilon_J}{n\sigma v_T} \qquad (3.6)$$

Then, in terms of the departure coefficients $b_J = n_J/n_J^*$, the population equation becomes

$$b_J\, (a_J + 1) = b_{J+1}\, a_{J+1}\, \frac{n_{J+1}^*}{n_J^*} + 1 \qquad (3.7)$$

This equation can be readily solved by changing the dependent variable to $a_J b_J$. For $J > 1$, the result is

$$a_J b_J = \sum_{J'=J}^{\infty} \frac{n_{J'}^*}{n_J^*} \prod_{J''=J}^{J'} \frac{a_{J''}}{1 + a_{J''}} \tag{3.8}$$

The ground state population is then given by

$$b_0 = b_1 a_1 \frac{n_1^*}{n_0^*} + 1 \tag{3.9}$$

In view of the approximate form of the cross-section used in obtaining the solution (3.8), considerable simplification is warranted. For simplicity, assume $J \gg 1$ so that

$$\begin{aligned} A_J &= A_0 J^3 \\ E_J &= E_0 J^2 \end{aligned} \tag{3.10}$$

where, for CO, $A_0 = 1.118 \times 10^{-7}$ s^{-1} and $E_0/k = 2.765$ K. Define y and J_T by:

$$y \equiv \frac{E_J}{kT} = \frac{E_0 J^2}{kT} \equiv \frac{J^2}{J_T^2} \tag{3.11}$$

For $kT \gg E_0$, the partition function is simply $Z = J_T^2$. The energy difference ΔE_J between levels J and J-1 is about $2E_0 J$ so that

$$\Delta E_J/kT = 2y/J \tag{3.12}$$

The quantity a_J defined in equation (3.6) can be expressed

$$a_J = \frac{J}{4} y \frac{n_{cr}}{n} \epsilon_J \tag{3.13}$$

where

$$n_{cr} \equiv 8 \frac{J_T^2 A_0}{\sigma v_T} \tag{3.14}$$

is the density of hydrogen nuclei at which collisional de-excitation becomes important in an optically thin gas (HM).

First, consider the high density limit in which $a_J \to 0$ and the levels are nearly in LTE. Treating both a_J and J^{-1} as small and keeping terms to 2nd order in small quantities, we find that the solution (3.8) reduces to

$$b_J \simeq \frac{1 + (n_{cr}\,\epsilon_J/n)\,y}{1 + \frac{1}{2}(n_{cr}\epsilon_J/n)y^2} \tag{3.15}$$

Next consider the low density limit in which $a_J \to \infty$, so that

$$a_J\, b_J \to \sum_{J'=J}^{\infty} \frac{n_{J'}}{n_J}^{*} \tag{3.16}$$

Replacing the sum by an integral, we find for $J \gg 1$

$$b_J \simeq \frac{1}{\frac{1}{2}(n_{cr}\epsilon_J/n)y^2} \tag{3.17}$$

A generalization which is valid at $J = 0$ as well is

$$b_J \simeq \frac{1}{b_o^{-1} + \frac{1}{2}(n_{cr}\,\epsilon_J/n)\,y^2} \tag{3.18}$$

There is considerable latitude in combining equations (3.15) and (3.18) into a general approximation for all densities. Since the quantum mechanical calculation of the cross-sections shows that σ decreases slowly with J, we expect that n_{cr} will increase slowly with y. Hence we make the replacement

$$\frac{n_{cr}\,\epsilon_J}{n} \to wy^{\beta} \tag{3.19}$$

and treat w and β as parameters to be determined by comparison with the numerical results for the level populations presented in §II. A simple expression which reduces to equations (3.15) and (3.18) in the appropriate limits is

$$b_J = \frac{1 + wy^{1+\beta}}{b_o^{-1} + \frac{1}{2}wy^{2+\beta}(1 + wy^{1+\beta})}\,. \tag{3.20}$$

At high densities, $b_o \simeq 1$, as indicated in equation (3.15).

With this expression as a foundation, we have developed the following approximation for the departure coefficients in the optically thin case by trial-and-error comparison with the detailed numerical results:

$$b_J = \left[\frac{1 + wy^{1.3}}{b_o^{-1} + \frac{1}{2} wy^{2.3} (1 + wy^{1.3})} \right] \frac{1}{f} \tag{3.21}$$

$$b_o = (1 + \frac{2}{3} w^{0.83})^{1/2} \tag{3.22}$$

$$f = (1 + \frac{0.55\ y^{2.2}}{T_3^{-0.2} + 6w^{-0.75}})^2 \tag{3.23}$$

$$w = \frac{2.75\ T_3^{\alpha}}{n_6} \tag{3.24}$$

$$\alpha = 0.74 + 0.16\ T_3^{1/2} \tag{3.25}$$

where $n_6 \equiv n/(10^6\ cm^{-3})$ and $T_3 \equiv T/(10^3\ K)$. The factor f has been inserted to reduce the populations at large values of J, thereby accounting for the inefficiency of collisions with large ΔJ. There is an upper bound on b_o determined by the condition that all CO molecules be in the J=0 level, which gives $b_o < Z = J_T^2$; however, this limit is reached only for densities below that at which the above approximation is valid (see below). At $T_3 = 1$ and $J = J_T = 19$, the value of w in equation (3.24) corresponds to $n_{cr} = 2.8 \times 10^6\ cm^{-3}$, or $\sigma = 4 \times 10^{-16}\ cm^2$. As mentioned above, this effective value of the cross-section is several times smaller than the total de-excitation cross-section.

This analytic approximation is remarkably accurate over a wide range of physical conditions. Let J_p be the rotational quantum number of the highest level which produces a line with an intensity within a factor 50 of the strongest line; if the strongest line is at J_m, then typically $J_p \sim 2J_m$. Comparison with the numerical results shows that our approximation is correct to within a factor 1.33 for $0 < J < J_p < 50$ over the range $2 \times 10^4\ cm^{-3} < n$ and $250\ K < T < 2000\ K$, except at low densities and high temperatures: at $n = 2 \times 10^5\ cm^{-3}$, the accuracy drops for $T > 1750$ K and is 1.4 at 2000 K; at $n = 2 \times 10^4$ K, the accuracy drops for $T > 1000$ K and is 2.0 at 2000 K.

The accuracy of the approximation was checked at 5 densities, $n = 2 \times 10^4$ cm^{-3}, 2×10^5 cm^{-3}, ...2×10^8 cm^{-3}, and at intervals of 250K from 250 K to 2000 K. At T = 100 K, the accuracy is 1.5 for $n > 2 \times 10^4$ cm^{-3}.

The approximation developed here is readily extended to the case of finite optical depth in the lines by multiplying the value of w given in equation (3.24) by the escape probability ϵ_J (see HM). We have not attempted to assess the accuracy of this procedure, however.

IV. POPULATION INVERSION

Population inversions result in maser action and can produce extremely intense sources of radiation. Because of high abundance of CO in molecular clouds, inversion of CO levels could be particularly important. Goldsmith (1972) suggested that the J = 1 level of CO could become inverted because collisions from J = 0 to J = 2 occur at a rate comparable to those from J = 0 to J = 1, whereas radiative transitions from J = 2 to J = 1 occur much more rapidly than from J = 1 to J = 0. In a detailed calculation including radiative transfer, Leung and Liszt (1976) found that at 40 K the 1 → 0 transition became suprathermal (excitation temperature > kinetic temperature) but not inverted. Because of the lower optical depth in ^{13}CO, much higher excitation temperatures were achieved in ^{13}CO than in ^{12}CO. Actual inversions were predicted in the CS molecule at this temperature (Liszt and Leung 1977). Calculations of the populations in cyanoacetylene (HC_3N), which is a linear molecule like CO, indicate that the 1 → 0 transition can be inverted for 10^3 $cm^{-3} \lesssim n \lesssim 10^5$ cm^{-3}, whereas the 2 → 1 transition is inverted over a narrower range (Morris et al. 1976). The latter authors claimed evidence for a weak cyanoacetylene maser in Sgr B2.

Using the detailed numerical calculations discussed in §II, we have made a systematic search for population inversions in CO over a wide range of temperatures and densities. We have not included any radiative transfer effects, because that would entail making additional assumptions about the geometry of the source and the intensity of the background radiation. We find that the 1 → 0 transition can be inverted for T ~ 50 K over a narrow range of densities; as the temperature is increased, the range of densities over which an inversion occurs increases and higher levels become inverted as well. The mechanism for producing the inversions is a direct generalization of that suggested by Goldsmith (1972): collisional rates vary more slowly with J than do the radiative rates, so it is possible for molecules to become trapped at high J.

Our results are summarized in Table 2 and Figure 2. The magnitude of the inversion $n_J g_J^{-1}/(n_{J-1}\, g_{J-1}^{-1})$ and the "saturation column density" N_{sat} are presented as a function of J, $n(H_2)$, and T. When the CO column density equals N_{sat}, the optical depth in the J → J-1 transition is -1. For $N(CO) < N_{sat}$, our optically thin approximation is valid but the amplification is small. For $N(CO) > N_{sat}$, the amplification could be large in principle, but a detailed radiative transfer calculation would be needed to make certain. The value of N_{sat} is determined by the optical depth τ_J in the J → J-1 transition. At line center we have

$$\tau_J = N_{J-1} \frac{g_J}{g_{J-1}} \frac{\lambda^3 A_J}{8\pi^{3/2}\Delta v} \left(1 - \frac{N_J\, g_{J-1}}{N_{J-1}\, g_J}\right) \qquad (4.1)$$

where N_J is the column density in level J. The line width Δv is taken to be the half width to 1/e points of the line, expressed in velocity units; for a thermal profile, $\Delta v = 12.9\ (T/A)^{1/2}$ km s^{-1}, where A is the molecular weight. Noting that $A_J = \mu^2\, \lambda^{-3}$, where μ is the dipole moment, we can solve equation (4.1) for N(CO) when $\tau = -1$ and obtain

$$N_{sat} = 2.74 \times 10^{13} \left[\frac{N_{J-1}}{N(CO)} \frac{J}{(2J-1)\sqrt{T}} \left(\frac{N_J}{N_{J-1}} \frac{g_{J-1}}{g_J} - 1\right)\right]^{-1} \text{ cm}^{-2} \quad (4.2)$$

where the ratios $N_{J-1}/N(CO)$ and N_J/N_{J-1} may be obtained from the calculations described in §II. The values for N_{sat} given in Table 2 are minimum values because we adopted the minimum line width - the thermal width. CO has unusually large values of N_{sat} because of its small dipole moment.

The conditions required for a population inversion may be understood as follows. Let J_ℓ be the level at which n_J is a maximum; obviously, an inversion is possible only for $J < J_\ell$. If the density is too high, then the populations approach their LTE values and no inversion is possible. If either the density or the temperature is too low, then J_ℓ will drop below J and again no inversion is possible for level J. The upper limit on the density can be estimated from the approximation developed in §III; unfortunately, the lower limit occurs at a density too low for the approximation to be valid. Since an inversion is possible only for low values of J, the quantity $y = J^2/J_T^2$ is small and the factor f can be set equal to unity in equation (3.21). Hence b_J depends only on the two variables w and y, and not on n, T, and J separately. The condition that an inversion occur for a specified y can than depend only on w. Since an inversion is possible only for densities below some critical value (which depends on T), the condition must be a lower limit on w; i.e., we require $w > w_{crit}$ for an inversion. Inspection of Table 2 suggests $w_{crit} \approx 4$, which gives

$$n(H_2) \lesssim 10^{5.5}\, T_3^{\alpha} \text{ cm}^{-3} \quad (4.3)$$

as the condition for an inversion. At $T \sim 50$ K, the upper and lower limits on the density converge at $n(H_2) \sim 3 \times 10^4$ cm^{-3}; the numerical calculations show that an inversion is impossible for $T \lesssim 50$ K. As T increases above 50 K, J_ℓ rises so that higher levels become inverted as well.

As emphasized above, our calculation of population inversions is valid only in the optically thin limit, $N < N_{sat}$, which seemingly precludes large amplifications. However, if the CO is in a thin sheet, then our calculations may be directly applicable even if the amplification is large: in most directions one could have $N(CO) < N_{sat}$ so that the level populations are unaffected by radiative transfer, but when viewed edge-on the sheet could have $N(CO) \gg N_{sat}$, producing a source of high brightness. The optically thin limit may also be preserved if the gas has a large superthermal internal velocity dispersion. Such conditions are expected for interstellar shocks. Observations of regions containing interstellar shocks, with sufficient spatial resolution to resolve the shock thickness, could reveal regions of anomalously high brightness in the lower CO rotational lines. A possible example of such a region is IC 443 (De Noyer 1979a,b) where some components may be edge-on, although the excitation seems too small to produce inversion. Unfortunately, in Orion, the best-studied example of interstellar molecular shocks, the observed CO emission originates in gas which is too dense ($n[H_2] \sim 10^6$ cm^{-3}) to produce a population inversion.

Detailed calculations are required to determine if significant amplification can occur in actual interstellar shocks. Reference to Table 2 shows that relatively large column densities of warm gas are required to produce one e-folding in the intensity: $N(H) \sim 10^{20-21}$ cm^{-2} at $n(H_2) = 10^4$ cm^{-3} and $N(H) \sim 10^{21.5-22.5}$ cm^{-2} at $n(H_2) = 10^5$ cm^{-3}, under the assumption that $n(CO)/n \sim 10^{-4}$. If the emission occurs in a magnetic precursor to the shock (Draine 1980) then n is the pre-shock density; if the emission occurs in the shocked gas, then n is the shocked density, which is typically 10-30 times greater (HM).

V. OPTICALLY THIN COOLING RATES

Because of its relatively high abundance, CO is often an important coolant in molecular clouds (e.g., Dalgarno, et al 1975). We define the rotational cooling rate coefficient L_{rot} by setting $n\, n(CO)\, L_{rot}$ equal to the total CO rotational emission rate; assuming that the gas is optically thin, we have

$$n\, n(CO)\, L_{rot} = \sum_{J=1}^{\infty} n_J\, A_J\, \Delta E_J = 4\pi n(CO) \sum_{J=1}^{\infty} I_J \tag{4.1}$$

where ΔE_J is the energy difference between levels J and J-1 and I_J is defined in equation (2.7). HM obtained the approximate result

$$L_{rot} = \frac{4(kT)^2\, A_o}{n E_o [1 + (n_{cr}/n) + 1.5(n_{cr}/n)^{1/2}]} \tag{4.2a}$$

$$= \frac{\frac{1}{2}\, k\, T\, \sigma v_T}{1 + (n/n_{cr}) + 1.5\, (n/n_{cr})^{1/2}} \tag{4.2b}$$

where the equivalence of the two expressions follows from the definition of n_{cr}, equation (3.14). The factor 1/2 in equation (4.2b) is simply $n(H_2)/n$.

Using the numerical results discussed in §II, we find that this expression for the CO cooling rate is quite accurate. Setting

$$n_{cr} = 3.5 \times 10^6\, T_3^{2/3}\ cm^{-3}, \tag{4.3}$$

which corresponds to $\sigma = 1.6 \times 10^{-16}\ cm^2$ at $T_3 = 1$, we find an accuracy of 20% for $2 \times 10^4\ cm^{-3} < n < 2 \times 10^8\ cm^{-3}$ and 250 K < T < 2000 K. However, HM's numerical value for the critical density ($n_{cr} = 6 \times 10^5\, T_3^{1/2}\ cm^{-3}$) is almost an order of magnitude too low, primarily because they set σ equal to the total de-excitation cross-section of about $10^{-15}\ cm^2$; in addition, they used a thermal velocity appropriate for atomic hydrogen. This underestimate of n_{cr} would lead to an overestimate of the CO cooling at low densities by almost an order of magnitude.

In order to see how the σ in equations (3.14) and (4.2b) is related to the collisional rates presented in Table 1, we proceed as follows. In the low-density limit

$$L_{rot} = \frac{n(H_2)}{n} \sum_J \gamma_{J0}\, g_J\, e^{-E_J/kT}\, E_J \tag{4.4}$$

$$= \frac{1}{2} \frac{(kT)^2}{E_0} \int \gamma_{J0}\, y e^{-y}\, dy \tag{4.5}$$

For $2 < J < J_T$, the results in Table 1 can be approximated as $\gamma_{J0} = \gamma_{20}(2/J)^2$; for $J = 1$ and $J > J_T$, γ_{J0} is smaller. Evaluation of the integral gives $L_{rot} = 2kT\gamma_{20}C$, where the factor C allows for the smaller values of γ_{J0} for $J > J_T$ ($y > 1$); we somewhat arbitrarily set $C = (1 - e^{-1}) = 0.6$. Comparing this result with equation (4.2b) in the limit $n << n_{cr}$, we obtain

$$\sigma v_T = 2.4\ \gamma_{20} \tag{4.6}$$

If allowance is made for the mass difference between He and H_2, one finds that $\gamma_{20} = 3.2 \times 10^{-11}\ T_3^{1/3}\ cm^3\ s^{-1}$ for H_2. Finally, inserting these results into the defirition (3.1[illegible]) of n_{cr} gives $n_{cr} = 4.3 \times 10^6\ T_3^{2/3}\ cm^{-3}$, quite close to the value found above. Equation (4.6) should allow one to estimate n_{cr} for molecules other than CO, provided their excitation rates behave similarly.

Finally, we note that equation (4.5) applies only in a gas of molecular hydrogen. Behind fast shocks, relatively large concentrations of atomic hydrogen can build up (Hollenbach and McKee 1980). If $x_2 = n(H_2)/n$, then in the presence of atomic hydrogen the critical density (eq. 3.14) becomes

$$n_{cr} = \frac{4\ J_T^2\ A_0}{\sigma v_T \left[x_2 + \frac{\sigma_H}{\sigma}\,(1 - 2x_2)\,\sqrt{2}\right]}, \tag{4.7}$$

where σ_H is the effective cross-section for rotational excitation in collisions of atomic hydrogen with CO. In a fully molecular gas, $x_2 = \frac{1}{2}$ and equation (3.14) is recovered.

VI. CONCLUSION

The numerical and analytic results we have presented for the rotational spectrum of CO should be useful in interpreting observations of interstellar CO emission from warm molecular gas and in generating theoretical models of shocks in molecular clouds. The results are valid for optically thin CO which is collisionally excited by H_2 collisions; infrared pumping has been ignored. The analytic results can be extended to the optically thick case in an approximate fashion by using the escape probability formalism.

An important result of our analysis is that population inversions in the lower rotational levels of CO can be expected to occur in warm molecular gas with density in the range $n(H_2) \sim 10^{3-5}$ cm^{-3}. The number of levels for which an inversion occurs the column density required for significant amplification both increase with temperature (see Table 2 and Figure 8). Interstellar shocks appear to be promising as sites of CO masers. The expression for the CO cooling rate obtained by HM has been verified. However, we find that the effective cross-section which determines the cooling rate is significantly smaller than they assumed ($\sigma \sim 4 \times 10^{-16}$ cm^2 rather than 10^{-15} cm^2), and that the cooling rate at low densities is correspondingly reduced. The effective excitation cross-sections for OH and H_2O, the other dipolar molecules which are important coolants, are probably also less than the value 10^{-15} cm^2 assumed by HM; however, since the ΔJ required to obtain a given energy difference is much smaller for these molecules than for CO, we anticipate their effective cross-sections are closer to 10^{-15} cm^2 than that of CO.

ACKNOWLEDGEMENTS

C.F.M. gratefully acknowledges numerous conversations with D. Hollenbach. His research is supported by NSF grant AST 79-23243. J.W.V.S. and D.M.W. are supported in part by NASA grant NGR 05-003-511. S.G. acknowledges partial support from NASA grant NSG 7105.

REFERENCES

Brechignac, P., Picard-Bersellini, A., Charneau, R., and Launay, J.M. 1980, Chem. Phys. 53, 165.

Dalgarno, A., de Jong, T., Oppenheimer, M., and Black, J.H. 1975, Ap. J. (Letters), 192, L37.

de Jong, T. 1973, Astr. Ap., 26, 297.

De Noyer, L.K. 1979a, Ap. J. (Letters), 228, L41.

_____. 1979b, Ap.J. (Letters), 232, L165.

De Pristo, A.E., Augustin, S.D., Ramaswamy, R., and Rabitz, H. 1979, J. Chem. Phys., 71, 850.

Draine, B. 1980, Ap. J., (in press).

Goldflam, R., Green S., and Kouri, D.J. 1977, J. Chem. Phys., 67, 4149.

Goldsmith, P.F. 1972, Ap. J., 176, 597.

Green, S. 1979, Chem. Phys., 40, 1.

Green, S. and Chapman, S. 1977, J. Chem. Phys., 67, 2317.

Green, S. and Thaddeus, P. 1976, Ap. J., 205, 766.

Green, S. and Thomas, L.D. 1980, J. Chem. Phys. 73, 5391.

Hollenbach, D.J. and McKee, C.F. 1979, Ap. J. Suppl., 41, 555 (HM).

_____. 1980, Ap. J. (Letters), 241, L47.

Leung, C.M., and Liszt, H.S. 1976, Ap. J., 208, 732.

Liszt, H.S. and Leung, C.M. 1977, Ap. J., 218, 396.

Morris, M., Turner, B.E., Palmer, P., and Zuckerman, B. 1976, Ap. J., 205, 82.

Nerf, R.B. and Sonnenberg, M.A. 1975, J. Molec. Spectros., 58, 474.

Storey, J.W.V., Watson, D.M., Townes, C.H., Haller, E.E., and Hansen, W.L. 1981, Ap. J. 247 (in press).

REFERENCES

Thomas, L.D., Kraemer, W.P., and Diercksen, G.H.F. 1980, Chem. Phys., 51, 131.

Watson, D.M., Storey, J.W.V., Townes, C.H., Haller, E.E. and Hansen, W.L. 1980, Ap. J. (Letters) 239, L129.

Table 1

He-CO Collisional Rate Coefficients [a]

L	γ_{LO} ($cm^3\ s^{-1}$)						
	100 K	250 K	500 K	750 K	1000 K	1500 K	2000 K
1	1.72(-11)	2.31(-11)	2.53(-11)	2.65(-11)	2.75(-11)	2.92(-11)	3.07(-11)
2	6.89(-12)	1.28(-11)	1.74(-11)	2.00(-11)	2.19(-11)	2.49(-11)	2.72(-11)
3	4.72(-12)	7.35(-12)	8.78(-12)	9.43(-12)	9.86(-12)	1.05(-11)	1.10(-11)
4	1.47(-12)	2.89(-12)	4.56(-12)	5.61(-12)	6.33(-12)	7.31(-12)	7.97(-12)
5	1.54(-12)	3.07(-12)	4.38(-12)	5.07(-12)	5.51(-12)	6.06(-12)	6.40(-12)
6	7.29(-13)	1.32(-12)	1.92(-12)	2.39(-12)	2.76(-12)	3.28(-12)	3.63(-12)
7	4.26(-13)	1.15(-12)	2.04(-12)	2.65(-12)	3.07(-12)	3.61(-12)	3.94(-12)
8	2.60(-13)	6.52(-13)	9.83(-13)	1.22(-12)	1.41(-12)	1.71(-12)	1.92(-12)
9	1.27(-13)	4.87(-13)	1.00(-12)	1.42(-12)	1.76(-12)	2.24(-12)	2.55(-12)
10	7.81(-14)	3.22(-13)	5.76(-13)	7.34(-13)	8.55(-13)	1.04(-12)	1.18(-12)
11	3.99(-14)	2.34(-13)	5.27(-13)	7.83(-13)	1.01(-12)	1.38(-12)	1.65(-12)
12	2.25(-14)	1.56(-13)	3.49(-13)	4.79(-13)	5.76(-13)	7.16(-13)	8.12(-13)
13	1.19(-14)	1.12(-13)	2.92(-13)	4.43(-13)	5.84(-13)	8.38(-13)	1.05(-12)
14	6.20(-15)	7.16(-14)	2.09(-13)	3.17(-13)	4.01(-13)	5.26(-13)	6.13(-13)
15	3.27(-15)	5.08(-14)	1.67(-13)	2.66(-13)	3.54(-13)	5.16(-13)	6.63(-13)
16	1.66(-15)	3.18(-14)	1.23(-13)	2.08(-13)	2.79(-13)	3.89(-13)	4.73(-13)
17	8.14(-16)	2.15(-14)	9.56(-14)	1.67(-13)	2.28(-13)	3.37(-13)	4.33(-13)

Table 1 (continued)

L	γ_{LO} (cm^3 s^{-1})						
	100 K	250 K	500 K	750 K	1000 K	1500 K	2000 K
18	3.81(-16)	1.35(-14)	7.08(-14)	1.33(-13)	1.87(-13)	2.77(-13)	3.51(-13)
19	1.81(-16)	8.82(-15)	5.33(-14)	1.03(-13)	1.47(-13)	2.21(-13)	2.84(-13)
20	9.09(-17)	5.51(-15)	3.98(-14)	8.39(-14)	1.26(-13)	1.99(-13)	2.62(-13)
21	3.84(-17)	3.34(-15)	2.86(-14)	6.38(-14)	9.76(-14)	1.54(-13)	2.00(-13)
22	2.55(-17)	2.12(-15)	2.15(-14)	5.21(-14)	8.41(-14)	1.42(-13)	1.92(-13)
23	5.74(-18)	1.31(-15)	1.62(-14)	4.15(-14)	6.75(-14)	1.11(-13)	1.41(-13)
24	1.13(-18)	7.24(-16)	1.15(-14)	3.26(-14)	5.68(-14)	1.03(-13)	1.43(-13)
25	1.52(-19)	3.86(-16)	8.29(-15)	2.52(-14)	4.47(-14)	7.97(-14)	1.06(-13)
26	8.52(-20)	2.47(-16)	6.10(-15)	1.98(-14)	3.68(-14)	7.03(-14)	9.95(-14)
27	4.83(-20)	1.54(-16)	4.31(-15)	1.50(-14)	2.88(-14)	5.69(-14)	8.17(-14)
28	2.14(-20)	9.10(-17)	3.09(-15)	1.16(-14)	2.34(-14)	4.87(-14)	7.19(-14)
29	1.35(-20)	5.80(-17)	2.18(-15)	8.85(-15)	1.89(-14)	4.24(-14)	6.54(-14)
30	6.76(-21)	3.51(-17)	1.57(-15)	6.94(-15)	1.54(-14)	3.60(-14)	5.62(-14)
31	8.99(-22)	1.86(-17)	1.12(-15)	5.49(-15)	1.27(-14)	3.00(-14)	4.59(-14)
32	4.54(-22)	1.09(-17)	7.96(-16)	4.37(-15)	1.10(-14)	2.94(-14)	4.93(-14)

Note to Table 1

(a) Rate coefficients for He-CO collisions are given. H_2-CO rate coefficients are obtained by multiplying values in this table by 1.37.

Table 2

Population Inversions and "Saturation" Column Densities for CO

J		1		2		3		4	5	6	7
T[a]	$n(H_2)$[a]	10^4	10^5	10^4	10^5	10^4	10^5	10^5	10^5	10^5	10^5
100		1.21[b]	---	---	---	---	---	---	---	---	---
		1.41(16)[b]									
250		1.257	1.002	1.043	---	---	---	---	---	---	---
		3.79(16)	1.09(19)	8.93(16)							
500		1.221	1.007	1.228	1.012	---	1.014	1.001	---	---	---
		1.03(17)	7.86(18)	4.08(16)	2.06(18)		1.19(18)	1.10(19)			
750		1.194	1.008	1.286	1.015	1.001	1.021	1.021	1.004	---	---
		1.91(17)	1.15(19)	5.4(16)	2.85(18)	1.10(19)	1.32(18)	9.73(17)	4.59(18)		
1000		1.174	1.008	1.307	1.016	1.086	1.023	1.028	1.022	---	---
		3.00(17)	1.60(19)	7.24(16)	3.91(18)	1.32(17)	1.73(18)	1.06(18)	1.05(18)		
1500		1.147	1.008	1.308	1.016	1.187	1.024	1.031	1.035	1.026	---
		5.69(17)	2.69(19)	1.18(17)	6.47(18)	9.94(16)	2.34(18)	1.55(18)	1.09(18)	1.17(18)	
2000		1.130	1.007	1.295	1.015	1.240	1.023	1.032	1.038	1.037	1.022
		8.86(17)	3.88(19)	1.73(17)	9.36(18)	1.09(17)	4.01(18)	2.17(18)	1.40(18)	1.15(18)	1.62(18)

Notes to Table 2:

(a) $n(H_2)$ is in cm^{-3}, T in K.

(b) The upper entry for each $(T, n(H_2), J)$ is the population inversion $n_J g_{J-1}/n_{J-1} g_J$; the lower is the saturation column density N_{sat} in cm^{-2}.

Figure Captions

Figure 1 (a-g) Line emission coefficient I_J for the CO rotational transitions $J \rightarrow J-1$, as a function of J for several temperatures and molecular hydrogen densities $n(H_2)$. The I_J distributions come from computer solution of the statistical equilibrium equations, as discussed in §II. Also shown, for comparison, are the I_J distributions resulting from thermal equilibrium (LTE) level populations.

Figure 2 Population inversion $n_J g_{J-1}/n_{J-1} g_J$ as a function of temperature and molecular hydrogen density for the J = 1 and J = 2 states of CO. These curves were generated using computer solutions of the statistical equilibrium equations, as discussed in §II.

Authors' Addresses

Sheldon Green:
NASA Institute for Space Studies
2880 Broadway
New York, NY 10025

Christopher F. McKee and Dan M. Watson:
Department of Physics
University of California
Berkeley, CA 94720

J.W.V. Storey:
Anglo-Australian Observatory
P.O. Box 296
Epping, N.S.W. 2121, Australia

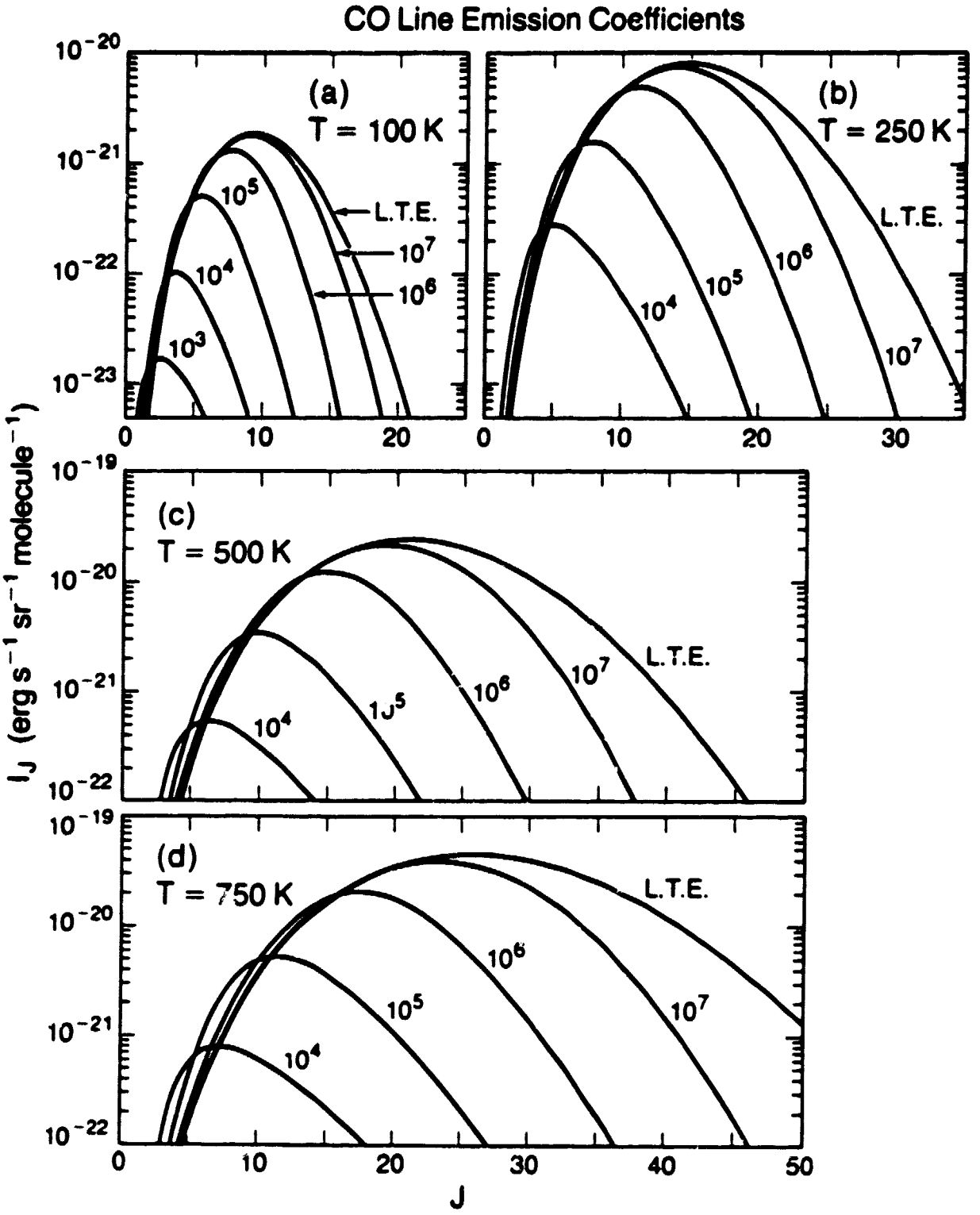
CO Line Emission Coefficients
(a)
T = 100 K
(b)
T = 250 K
(c)
T = 500 K
(d)
T = 750 K
L.T.E.
10^3
10^4
10^5
10^6
10^7
I_J (erg s^{-1} sr^{-1} molecule^{-1})
J

Figure 1 a - d

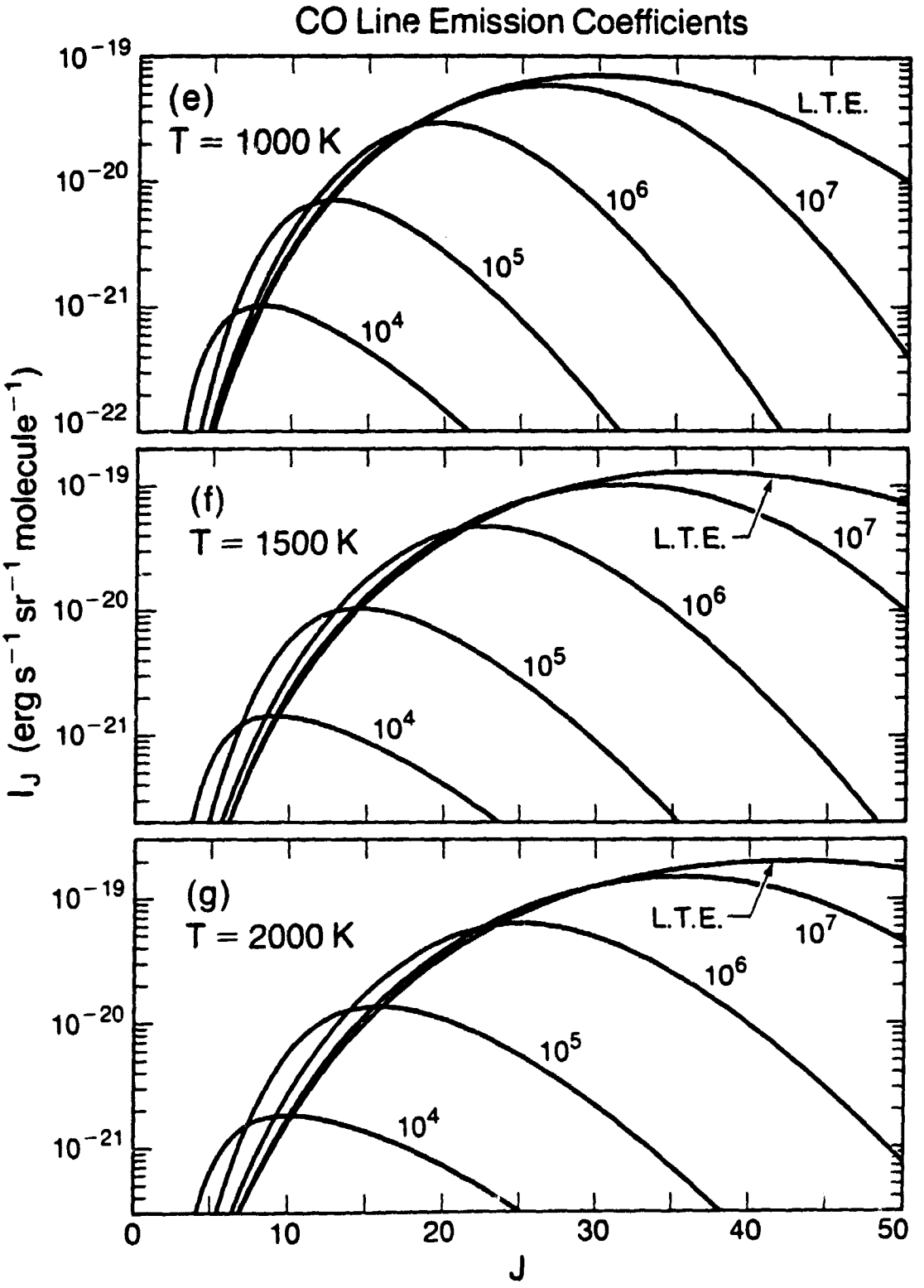
CO Line Emission Coefficients
(e)
T = 1000 K
(f)
T = 1500 K
(g)
T = 2000 K
L.T.E.
10^7
10^6
10^5
10^4
10^-19
10^-20
10^-21
10^-22
I_J (erg s^-1 sr^-1 molecule^-1)
0
10
20
30
40
50
J

Figure 1 e - g

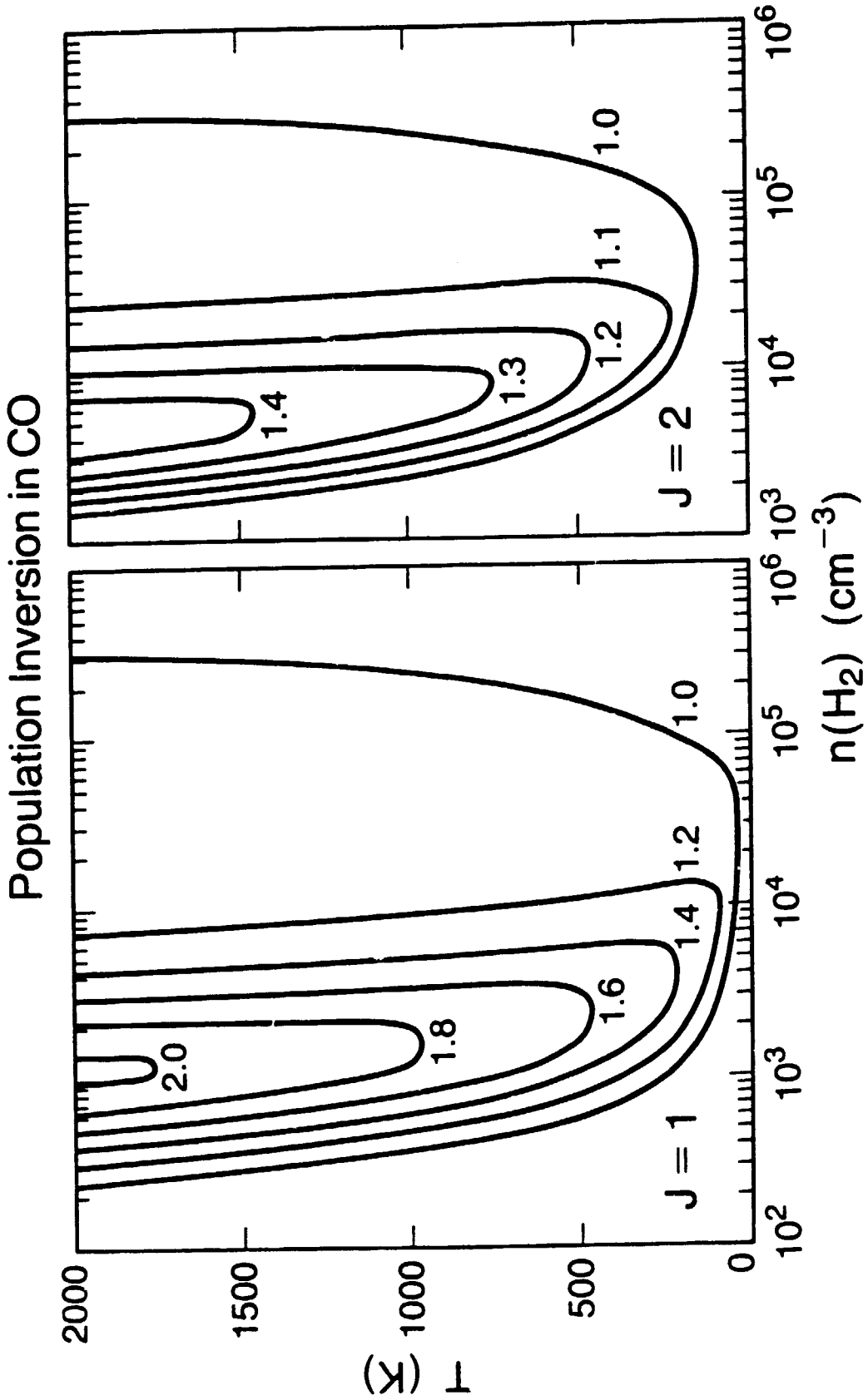
Population Inversion in CO
T (K)
2000
1500
1000
500
0
J = 1
2.0
1.8
1.6
1.4
1.2
1.0
J = 2
1.4
1.3
1.2
1.1
1.0
10^2
10^3
10^4
10^5
10^6
$n(H_2)$ (cm^{-3})

Figure 2